Fusion Technology

ISSN: 0748-1896 (Print) (Online) Journal homepage: https://www.tandfonline.com/loi/ufst19

Embrittlement of 2 1/4Cr-1Mo Steel by Lithium and a Lead-Lithium Liquid

G.R. Edwards, D.K. Matlock & B.A. Eberhard

To cite this article: G.R. Edwards, D.K. Matlock & B.A. Eberhard (1985) Embrittlement of 2 1/4Cr-1Mo Steel by Lithium and a Lead-Lithium Liquid, Fusion Technology, 8:1P2A, 937-943, DOI: 10.13182/FST85-A40154

To link to this article: https://doi.org/10.13182/FST85-A40154

EMBRITTLEMENT OF 2 1/4Cr-1Mo STEEL BY LITHIUM AND A LEAD-LITHIUM LIQUID

G.R. Edwards, D.K. Matlock, and B.A. Eberhard
Department of Metallurgical Engineering
Colorado School of Mines
Golden, Colorado 80401

ABSTRACT

The embrittlement of 2 1/4Cr-1Mo steel by lithium or lead-lithium liquids can occur when loading conditions and microstructural strengthening effects limit plastic relaxation at points of high stress, and a critical liquid metal induced embrittlement (LMIE) stress is reached. This paper presents the LMIE results of both constant displacement rate uniaxial tensile testing and fatigue crack propagation studies. The temperature for the onset of LMIE susceptibility at a given localized strain rate is shown to be predictable based on a critical value of flow stress, calculated by means of the Zener-Holloman parameter.

INTRODUCTION

Phenomenology of LMIE

Liquid metal induced embrittlement (LMIE) is the susceptibility to brittle fracture which can occur when normally ductile metals are stressed in tension in the presence of specific liquid metals[1]. Distinguishing characteristics of LMIE are: 1) existence of an applied stress sufficient to cause microscopic plastic deformation, and 2) intimate contact on an atomic scale between the liquid and solid metal[2]. Simultaneous occurrence of these two conditions is necessary but not sufficient to cause embrittlement. Various parameters associated with the embrittlement test method, test environment and solid metal microstructure have a pronounced effect on LMIE susceptibility, and ultimately determine the extent to which it occurs[3].

LMIE has been shown to occur in systems subjected to substantial tensile stress components, either directly applied or residual, and is considered a low temperature phenomenon with respect to the melting point of the embrittling metal[4,5]. In most cases, LMIE occurs over a well defined temperature range[3] and results of uniaxial tensile testing give rise to a reduction in fracture stress and a ductility "trough". The onset of a loss in ductility with increasing temperature generally occurs at or near the melting point of the embrittling metal. With a further increase in temperature, recovery of ductility depends on stress state, strain rate, liquid metal composition and solid metal microstructure. The width and depth of the ductility trough directly reflect the severity of the LMIE. For example, both the depth of the trough and the temperature for ductility recovery increase with strain rate[6].

Another major environmental influence of LMIE is chemical composition of the embrittling metal. Alloying a pure embrittling metal can either increase or decrease its embrittlement potential[7]. When alloying is observed to intensify embrittlement, the increase in embrittlement susceptibility is believed to be the result of enhanced wetting of the solid metal by the liquid metal alloy. This is achieved by: 1) the increased ability of the liquid metal to penetrate the oxide film at the solid/liquid metal interface, or 2) a decrease in surface tension of the liquid metal[8].

The intrinsic microstructural strength of an alloy, derived from its composition and process history, dominates its embrittlement susceptibility. For a given temperature and strain rate, material strength is determined by metallurgical factors such as grain size, phase composition and distribution, and degree of cold work. Variations in these parameters which increase material strength will invariably increase the material's susceptibility to liquid metal induced embrittlement[9]. The influence material strength has on LMIE is considered in greater detail in the following discussion of proposed embrittlement models.

Mechanistic Explanations for LMIE

To date, no mechanistic model exists which can account for all the observed phenomena of LMIE. Models based on stress-induced dissolution[10], formation of a weakly bonded alloy zone

ahead of the crack tip[11] and easier nucleation and propagation of dislocations[12] have been proposed but none are universally accepted. The most frequently quoted explanation for LMIE is the adsorption-induced reduction in atomic bond strength model[13-16]. This model suggests that absorption of liquid metal atoms at a crack tip effectively reduces the bond strength of the solid metal atoms. In an attempt to quantify the brittle fracture associated with LMIE, researchers have applied the brittle-ductile fracture criteria as reviewed by Kelly, Tyson, and Cottrell[17]. They concluded that a crack propagates in a brittle manner only when the ratio of applied tensile stress σ_{app} to applied shear stress τ_{app} is greater than the ratio of fracture stress, σ_c, to plastic flow stress, τ_f [16].

$$\frac{\sigma_{app}}{\tau_{app}} > \frac{\sigma_c}{\tau_f} \Rightarrow \text{brittle fracture}$$

When the ratio of applied tensile stress to applied shear stress is less than the ratio of fracture stress to flow stress, plastic relaxation at the crack tip prevents the brittle extension of the crack, and ductile rupture intervenes.

Absorption of a liquid metal atom at a crack tip creates a change in bond strength of solid metal atoms exactly at the crack tip and thereby affects the magnitude of σ_c. Electron screening reduces the influence of the liquid metal atoms to several atom diameters[18] and allows τ_f, which is a bulk material property, to remain unaffected. The ability of absorbed atoms to influence σ_c and not τ_f has led to the interpretation of σ_c as an environmentally sensitive parameter and τ_f as a metallurgical structure-sensitive parameter[16]. If at a given temperature, absorption of a liquid metal decreases σ_c while not affecting τ_f, the ratio of σ_c/τ_f is decreased and a brittle fracture is favored. On the other hand, factors which increase τ_f will decrease the ratio of σ_c/τ_f and increase the LMIE susceptibility. Either metallurgical strengthening mechanisms or an increase in the strain rate can increase τ_f. Increasing τ_f will cause the ductility recovery temperature, T_c, to be shifted to higher temperatures.

Application of Equation 1 is illustrated schematically in Figure 1. In this figure the assumed temperature dependencies of σ_c and τ_f for a metal susceptible to LMIE are illustrated. A discontinuity of σ_c is indicated to occur at a specific temperature, T_o. In this illustration, T_o is also the liquid metal melting temperature, T_m. Figure 1 suggests that, for all temperatures between T_o and T_c, LMIE is observed. The corresponding ductility trough for the metal is also illustrated in Figure 1. Note that the ductility recovery at any temperature above the liquid metal melting temperature, T_m (but less than T_c) should not be expected, based on the placement of the discontinuity of σ_c at T_m. Placement of the discontinuity in σ_c at the liquid metal melting temperature can be rationalized based on the results of Gordon[19]. Gordon has argued convincingly that liquid metal is readily transported to the crack tip, and must be assumed to be present there at any temperature above the melting temperature. Thus, the temperature for the discontinuity in σ_c cannot exceed the liquid metal melting temperature.

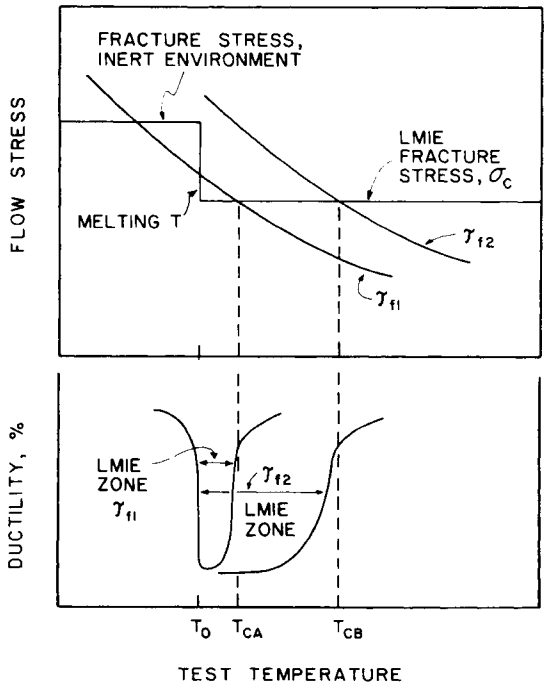

Figure 1. A schematic illustration of the temperature dependence of both LMIE fracture stress and flow stress for a metal exposed to an embrittling metallic liquid. Note that the flow stress is assumed to be monotonically decreasing with increasing temperature. Corresponding ductilities are also shown.

The behavior illustrated in Figure 1 cannot explain the observations that, with increasing test temperatures, the maximum loss in ductility due to LMIE has been observed at temperatures greater than the liquid melting temperature, i.e. $T_o > T_m$.[20]. One interpretation of this observation is shown in Figure 2, a schematic representation similar to Figure 1, in which τ_f is assumed to exhibit a maximum at a temperature above T_m. Specific metallurgical phenomena which could conceivably cause such

maxima in the flow stress are dynamic strain aging (solute-dislocation interactions) and secondary hardening. Both of these phenomena are commonly observed in hot tensile testing studies of 2 1/4Cr-1Mo steel.

A flow stress maximum, occurring at a temperature above the melting point of the embrittling liquid, could result in a ductility recovery from LMIE at any temperature $T_m<T<T_o$, as illustrated in Figure 2. Furthermore, factors which increase the flow stress, τ_f, (material strengthening or increased strain rate) should cause the entire ductility trough, $T_o<T<T_c$, to move to higher embrittling temperatures. Such an increase is also illustrated in Figure 2.

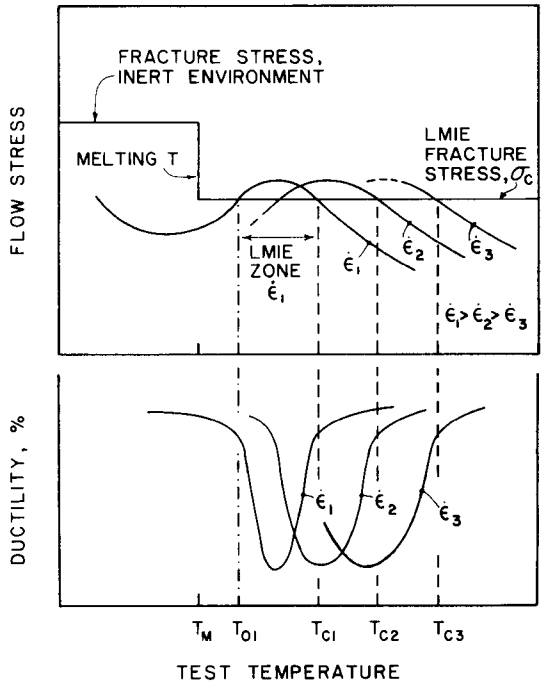

Figure 2. A schematic illustration of the temperature dependence of both LMIE fracture stress and ductility for a metal exposed to an embrittling metallic liquid. Note that the flow stress is assumed to maximize at a temperature above the melting temperature of the embrittling liquid. Corresponding ductilities are also shown.

In the remainder of this paper specific results for both tensile and fatigue testing of 2 1/4Cr-1Mo steel in lithium and in a lead-lithium liquid are presented. These results generally support the concepts illustrated in Figure 2; however, it will be shown that a flow stress maxima may not be the best measure of inhibited plastic relaxation at the crack tip.

TABLE I
EXPERIMENTAL HEAT TREATMENTS
LMIE of 2 1/4Cr-1Mo Steel in a
1 a/o Pb-99 a/o Li Liquid

HT-1: (Initial Treatment, All Specimens) Austenitized at 1300°C (20 min), Oil-Quenched (Simulation of Weld HAZ)

Heat Treatment	Condition	Comments	Temper Parameters*
HT-2	HT-1, plus 740°C temper for 10 hours	Represents severe temper (PWHT) at maximum code-allowable temperature	21.3×10^3
HT-3	HT-1, plus 695°C temper for 15.7 hours	Represents a minimal PWHT	20.5×10^3
MT-4	HT-1, plus 695°C temper for 121 hours	Represents PWHT near the minimal code allowable temperature and at approximately the same temper parameter at HT-2	21.4×10^3

*T.P. = T(20+log t) where T is in °K, t is in hours

TABLE II
CHEMICAL COMPOSITIONS
LMIE of 2 1/4Cr-1Mo Steel in a
1 a/o Pb-99 a/o Li Liquid

Steel Composition (w/o)

C	Mn	P	S	Cu	Si	Ni	Cr	Mo
0.06	0.38	0.013	0.024	0.27	0.22	0.19	2.25	0.92

Lithium Analysis (ppm)

Na	Fe	Ca	Si	N	Cl
75	<10	<60	<10	<30	<60

Lead Analysis (ppm)

Sn + Sb	Ag	Cu	Fe	As	Bi	Ni
50	0.5	3.0	3.0	0.2	1.3	3.0

RESULTS

Uniaxial Tensile Properties of 2 1/4Cr-1Mo Steel Exposed to a 1 a/o Pb-99 a/o Li liquid

Standard uniaxial tensile tests on 2 1/4Cr-1Mo steel, heat-treated to three microstructural conditions, and tested in both a 1 a/o Pb-99 a/o Li liquid and in an inert $NaNO_2$ salt, will be compared. Details of experimental procedures have been published elsewhere[20]. The heat treatments are summarized in Table 1. Note that heat treatment of all specimens began with a high temperature austenitizing treatment, designed to simulate the near heat-affected zone of a weld[21]. The chemical composition of the steel, the lead, and the lithium are given in Table II.

The uniaxial tensile flow stresses, determined at 5% strain, at a $1.1 \times 10^{-4} s^{-1}$ strain rate, and in the $NaNO_2$ salt bath, are plotted for each microstructural condition in Figure 3a. Corresponding unembrittled elongations at fracture (19mm gage length) are shown in Figure 3b. All conditions exhibited a maximum in flow stress at approximately 350°C, and the two weaker conditions (HT-3 and HT-4 specimens) exhibit an unembrittled ductility minimum at the strength maximum (≈350°C), as expected.

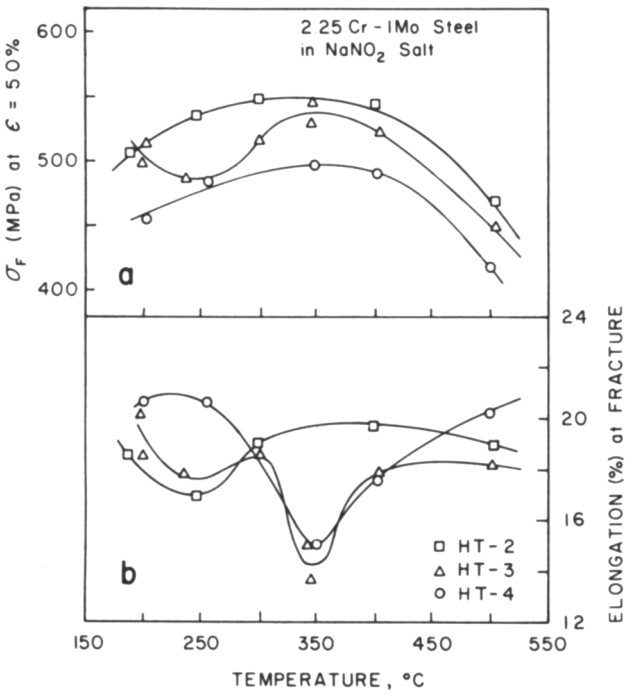

Figure 3. The mechanical properties for three heat treatments of 2 1/4Cr-1Mo steel, determined at 5% strain, $1.1 \times 10^{-4} s^{-1}$ initial strain rate, and in a protective $NaNO_2$ salt as a function of temperature. a) Uniaxial tensile flow stress b) Elongations at fracture.

When these specimens were tested at the same strain rate in a 1 a/o Pb-99 a/o Li liquid (T_m=180°C), a marked ductility loss at 250°C was observed. Fracture surfaces were typically intergranular when created under test conditions which maximized embrittlement. Example scanning electron fractographs of the HT-4 material, taken at ≈250°C of specimens tested both in the neutral $NaNO_2$ bath and in the embrittling liquid, are shown in Figure 4. Note the secondary intergranular cracking in the embrittled sample, while only ductile rupture microvoids are evident in the unembrittled sample. The embrittled elongations at fracture for all three microstructural conditions are shown in Figure 5. As expected, the severity of LMIE increased with the flow stress; however, the temperature for the embrittled ductility minima did not correspond with the temperatures of maximum strength. Rather, the ductility minima corresponded very

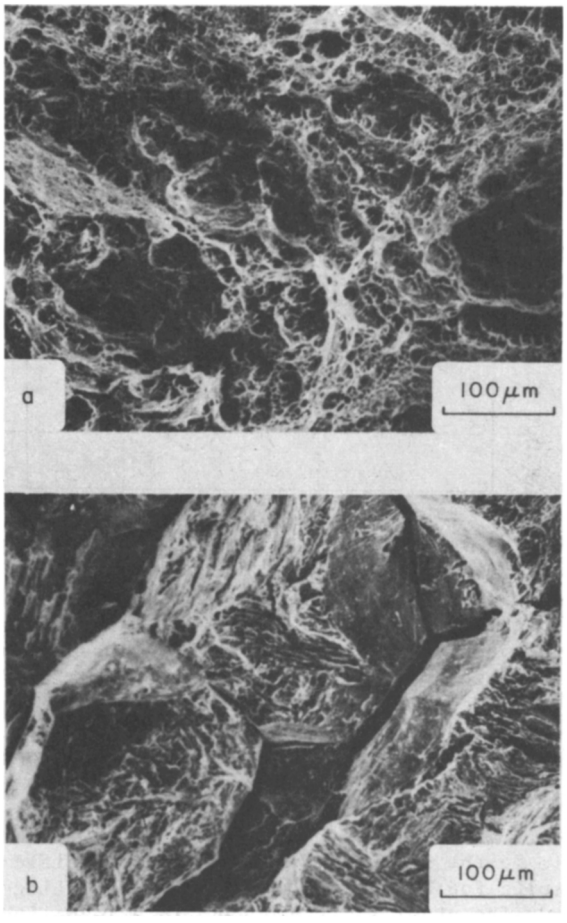

Figure 4. Scanning electron fractographs illustrating the fracture morphology of 2 1/4Cr-1Mo steel, heat treated to the HT-4 condition and fractured in: a) $NaNO_2$ salt at 255°C, and b) the 1 a/o Pb-99 a/o Li liquid at 252°C.

closely to the temperature where dynamic strain aging was a maximum. Also plotted in Figure 5 are the stress amplitudes of the strain aging serrations observed during the tests. Clearly, the magnitudes of the serrations increased with material strength, and maximized for all three microstructural conditions at 250°C. These results suggest that, while bulk flow stress measurements may determine relative magnitudes of LMIE susceptibility, they do not provide an adequate means of evaluating the temperature range of LMIE susceptibility, and the logic illustrated by Figure 2 is not complete.

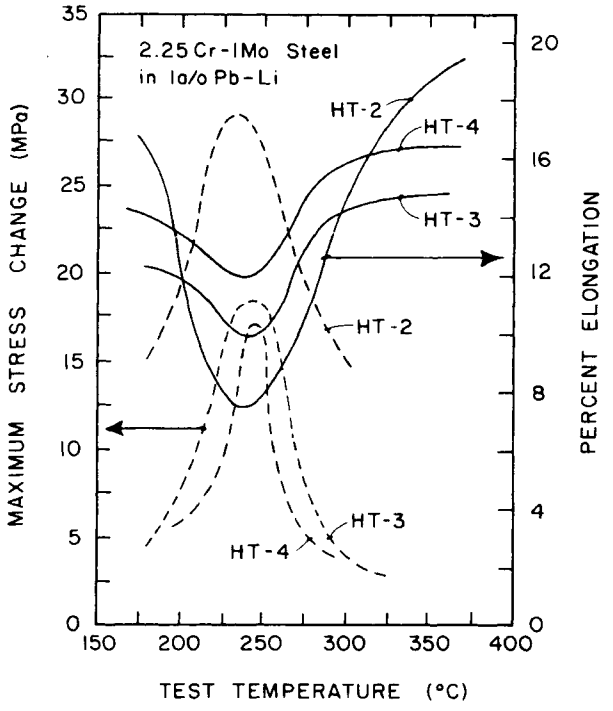

Figure 5. The ductilities observed for three heat treatments of 2 1/4Cr-1Mo steel. Specimens were fractured in tension while submerged in a 1 a/o Pb-99 a/o Li liquid at various temperatures. Also plotted are the amplitudes of the dynamic strain aging serrations observed during the tensile tests.

Apparently, bulk flow stress measurements do not adequately determine the resistance to plastic flow right at the crack tip, whereas, at least for 2 1/4Cr-1Mo steel, determining the temperature (at a given strain rate) which maximizes the dynamic strain aging also isolates the condition which most effectively immobilizes the dislocations at the crack tip. Consequently, the regime of maximum dynamic strain aging is also the regime of maximum LMIE susceptibility.

Fatigue Properties of 2 1/4Cr-1Mo Steel in Liquid Lithium

Enhancement of fatigue crack growth rates in 2 1/4Cr-1Mo steel submerged in liquid lithium has been attributed to LMIE[22]. The occurrence of LMIE was unique in that it was observed at temperatures up to 250°C above those observed for the uniaxial tensile data described above. A first consideration might be to assume that lithium alone reduced the fracture stress σ_c more than did the lead-lithium liquid previously discussed, so that embrittlement temperatures were increased. However, it will later be shown that the increased embrittlement temperature was simply a strain rate effect.

Fatigue crack growth rates measured on standard precracked fracture mechanics samples were obtained in both pure lithium and argon in the temperature range of 400°C (673K) to 600°C (873K) at loading frequencies between 0.067 and 20Hz. For these tests, the 2 1/4Cr-1Mo steel was heat treated to produce a large ferrite grain structure with spheroidized carbides, characteristic of a normalized and severely tempered steel.

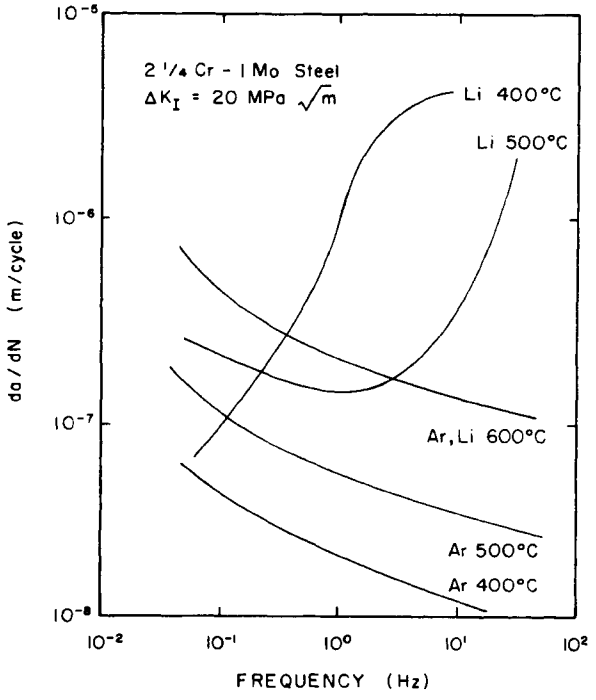

Figure 6. Crack growth rate, da/dN, plotted as a function of loading frequency for 2 1/4Cr-1Mo steel. Tests in argon and lithium (2000 ppm N) at a stress-intensity range of 20 MPa $\sqrt{m}$ and three temperatures are shown.

Experimental details, as well as a more detailed discussion of the results, are presented elsewhere[22]. A summary of results from this study are given in Figure 6. The major observation of this study, shown in Figure 6, was that crack propagation in lithium began to greatly exceed that in argon at a specific test frequency for a given temperature.

In fatigue crack growth, two characteristics of the tip of a propagating fatigue crack contribute to the significant increase in the embrittlement temperature: 1) The large, hydrostatic tensile component of the stress tensor which inhibits shear strain, and 2) the large and highly localized strain rates characteristic of fatigue crack propagation. Spencer et. al.[22] modeled the local strain at a fatigue crack tip and showed that loading frequencies of 0.067Hz to 20Hz correlate to local crack tip strain rates of $6 \times 10^{-4}s^{-1}$ to $0.2s^{-1}$. Consistent with the flow stress dependence discussed previously and illustrated in Figure 2, the increased strain rates correlated to increased local flow stresses at the crack tip and correspondingly increased temperatures, T_c, for the onset of LMIE.

The effects of frequency and thus local crack tip strain rate on the test temperature required for inducing LMIE during fatigue were analyzed by Spencer et. al.[22]. Consistent with Figure 2 their analysis assumed that a temperature independent LMIE fracture stress, σ_c, existed. Thus, to achieve LMIE as described in Equation 1, a critical crack tip flow stress was required. The flow stress of a metal depends on strain rate and temperature, and can be described by a Zener-Holloman analysis:

$$\tau_f = g(Z) = g(\dot{\epsilon} \exp(\Delta H/RT) \qquad (2)$$

where ΔH is the activation energy for plastic flow, $\dot{\epsilon}$ is the strain rate, and τ_f is the flow stress at a constant strain. In this analysis a critical τ_f corresponds to a critical value of Z. From the data of Klueh et. al.[23] ΔH was calculated to be 25 kcal/mole. With the observations that the effects of LMIE at 550°C were first observed at 6.7 Hz, a critical value of Z_c was calculated to be $7.62 \times 10^5 s^{-1}$. With a critical value of Z_c for LMIE, one can either calculate the strain rate at a given temperature, or calculate the temperature at a given strain rate where LMIE is observed. Spencer et. al.[22] used the critical Z_c to predict the critical loading frequencies (i.e. local crack tip strain rates) at temperatures of 400°C and 600°C. The resulting predictions correlated with experimental observations.

If the Zener-Holloman analysis is assumed to extend to the strain rates typical of uniaxial tensile testing, the critical temperature, T_c, for LMIE during tensile testing can be predicted. The tensile data previously considered were obtained at a strain rate of $1.1 \times 10^{-4}s^{-1}$. At this strain rate, application of the critical Z_c predicts that LMIE would be observed at 279°C. This prediction correlates well with the tensile data shown in Figure 5. One can thus conclude that LMIE susceptibility for 2 1/4Cr-1Mo steel can be predicted by utilizing empirical data and a Zener-Holloman analysis, and that strain rates from $10^{-4}s^{-1}$ to $0.2\ s^{-1}$ are appropriately analyzed by this method. It is also apparent that the LMIE resulting from exposure to a 1 a/o Pb-99 a/o Li liquid or to liquid lithium alone are not significantly different. This conclusion was also reached in the work of Eberhard, et. al.[20].

SUMMARY

The LMIE susceptibility of 2 1/4Cr-1Mo steel by either lithium or by a 1 a/o Pb-99 a/o Li liquid has been shown to be predictable by means of a Zener-Holloman analysis. Furthermore, the tensile data of Eberhard, et. al.[20] and the fatigue data of Spencer, et. al.[22] have been shown to be consistent with respect to a prediction of T_c, the maximum temperature at which LMIE is observed for a given strain rate. The Zener-Holloman analysis suggests that a critical value of flow stress, must exist at the crack tip before brittle crack extension in the presence of an embrittling liquid is possible. However, determination of the maximum bulk flow stress by means of uniaxial tensile testing did not accurately determine the LMIE temperature, T_c. Instead, determination of the temperature for maximum dynamic strain aging at a given strain rate proved a better measure of the LMIE temperature, T_c. These results suggest that the key to a thorough understanding of the LMIE phonemenon may reside in improved methods of quantifying the microdeformation characteristics of the material at the embrittled crack tip.

ACKNOWLEDGMENTS

D.K. Matlock acknowledges the support of the Materials Branch of the Basic Energy Science Division of the U.S. Department of Energy. G.R. Edwards and B.A. Eberhard are grateful for the support of Lawrence Livermore National Laboratory and the Electric Power Research Institute. The assistance of Mr. K. Jones is gratefully acknowledged.

REFERENCES

1. M.G. Nicholas and C.F. Old, "Review of Liquid Metal Embrittlement", J. Mat. Sci., 14, 1-4, (1979).

2. C.F. Old, "Liquid Metal Embrittlement of Nuclear Materials", J. Nuc. Mat., 92, 2, (1980).

3. W. Rostoker, J.M. McCaughey and H. Markus, "Embrittlement by Liquid Metals", Reinhold Pub. Corp., New York, (1960).

4. P. Gordon and H.H. An, "The Mechanisms of Crack Initiation and Crack Propagation in Metal-Induced Embrittlement of Metals", Met. Trans, 13A, 457, (1982).

5. J.C. Lynn, W.R. Warke, and P. Gordon, "Solid Metal-Induced Embrittlement of Steel", Mat. Sci. and Engr., 18, 51, (1975).

6. C.F. Old and P. Trevena, "Embrittlement of Zinc by Liquid Metals", J. Metal Sci., 13, 487, (1979).

7. M.H. Kamdar, "The Occurrence of Liquid-Metal Embrittlement", Phys. Stat. Sol., 4, 225, (1971).

8. R.J.K. Wassnik, "Wetting of Solid Metal Surfaces by Molten Metals", J. Inst. Metals, 95, 38, (1967).

9. N.S. Stoloff, R.G. Davis and T.L. Johnston, "Slip Character and Liquid Metal Embrittlement" in Environment - Sensitive Mechanical Behavior, Gordon and Breach, New York, pp. 613-655, (1966).

10. W.M. Robertson, "Embrittlement of Titanium by Liquid Cadmium", Met. Trans, 1, 2607, (1970).

11. N.I. Chavevskii, Soviet Mat. Sci., 1, 433, (1965).

12. S.P. Lynch, "Hydrogen Embrittlement and Liquid-Metal Embrittlement in Nickel Single Crystals", Scripta Met., 13, 1051, (1979).

13. N.S. Stoloff and T.L. Johnston, "Crack Propagation in a Liquid Metal Environment", Acta. Met., 11, 251, (1963).

14. M.J. Kelley and N.S. Stoloff, "Analysis of Liquid Metal Embrittlement from a Bond Energy Viewpoint", Met. Trans, 6A, 159, (1975).

15. A.R.C. Westwood and M.H. Kamdar, "Concerning Liquid Metal Embrittlement, Particularly of Zinc Monocrystals by Mercury", Phil. Mag., 8, 787, (1963).

16. M.H. Kamdar, Embrittlement by Liquid Metals, Pergamon Press, Ltd., Oxford, (1973).

17. A. Kelly, W.R. Tyson and A.H. Cottrell, "Ductile and Brittle Crystals", Phil. Mag., 15, 567, (1967).

18. E.A. Stearn, "Electron States Near Boundaries", Phys. Rev., 162, 565, (1967).

19. P. Gordon, "Metal-Induced Embrittlement of Metals - An Evaluation of Embrittle Transport Mechanism", Met. Trans., 9A, 267, (1978).

20. B.A. Eberhard, B.A. Mullinaux and G.R. Edwards, "The Susceptibility of 2 1/4Cr-1Mo Steel to Liquid Metal Embrittlement by Lithium - Lead Solutions", Liquid Metal Engineering and Technology, BNES, London, 337, (1984).

21. T.L. Anderson and G.R. Edwards, "The Corrosion Susceptibility of 2 1/4Cr-1Mo Steel in Lithium - 17.6 Wt. Pct. Lead Liquid", J. Mat. Energy Sys., 2, 16, (1981).

22. R.E. Spencer, D.K. Matlock and D.L. Olson", The Effects of Liquid Metal Embrittlement on High Temperature Fatigue of 2 1/4Cr-1Mo Steel in Liquid Lithium", J. Mat. Energy Sys., 4, 187, (1983).

23. R.L. Klueh and R.E. Oakes, Jr., J. Engr. Mat. and Tech., 98, 361, (1976).